Georgia Institute of Technology
Atlanta, Georgia 30332

ACTIVELY CONTROLLED SHAFT SEALS FOR AEROSPACE APPLICATIONS

Semiannual Status Report, July - December, 1993

NASA Research Grant NAG 3-974

Principal Investigator Richard F. Salant
College of Engineering
School of Mechanical Engineering

NASA Technical Officer: M.P. Proctor
NASA Lewis Research Center, MS SPT D-2
Space Vehicle Propulsion Branch

E25-666

I. INTRODUCTION

Since the last semiannual status report, effort has been directed toward documenting our work for publication. During this period two papers were prepared:

1. Wolff, P. J., and Salant, R. F., "Electronically controlled mechanical seal for aerospace applications - part II: transient tests," accepted for publication in Tribology Transactions, and for presentation at the 1994 STLE Annual Meeting.

2. Salant, R. F., and Wolff, P. J., "Development of an electronically controlled mechanical seal for aerospace applications," submitted for presentation at the 1994 SAE Aerospace Atlantic Conference and Exposition, and for publication in the SAE Transactions.

These two papers are incorporated into this report, and follow.

ELECTRONICALLY CONTROLLED MECHANICAL SEAL FOR AEROSPACE APPLICATIONS - PART II: TRANSIENT TESTS

Paul J. Wolff * and Richard F. Salant (Member, STLE)

School of Mechanical Engineering

Georgia Institute of Technology

Atlanta, Georgia 30332

(404) 894-3176

ABSTRACT

An electronically controlled mechanical seal for use as the purge gas seal in a liquid oxygen turbopump has been fabricated and tested under transient operating conditions. The thickness of the lubricating film is controlled by adjusting the coning of the carbon face. This is accomplished by applying a voltage to a piezoelectric actuator to which the carbon face is bonded. The seal has been operated with a closed-loop control system that utilizes either the leakage rate or seal face temperature as the feedback. Both speed and pressure transients have been imposed on the seal. The transient tests have demonstrated that the seal is capable of maintaining low leakage rates while limiting the face temperatures.

---

* Now at The Engineering Laboratory, Tennessee Valley Authority, Norris TN 37828.

KEY WORDS

mechanical seal, face seal, hydrostatic seal, gas seal, electronic control

NOMENCLATURE

e = error signal for controller, difference between set point and feedback

h_i = film thickness at inside radius

h_o = film thickness at outside radius

K_D = constant for control system, defined by Equation 3

K_I = constant for control system, defined by Equation 3

K_P = constant for control system, defined by Equation 3

O = output signal from controller

δ = coning, $h_o - h_i$

δ^* = nondimensional coning, δ/h_i

INTRODUCTION

Most mechanical seals are designed to operate, under steady state conditions, with a thin lubricating film between the faces of the seal. However, under off-design conditions, the lubricating film could break down and the seal faces could contact, resulting in high face

temperatures, high contact stresses, and high wear rates. To prevent face contact and promote reliability, controllable mechanical seals have recently been developed (1-4). In these seals, the film thickness is adjustable and can be increased under operating conditions for which face contact might occur.

In a previous study (5), a controllable gas seal for aerospace applications was examined under steady state operating conditions. Results from experiments were compared with those obtained from a mathematical model. During the steady state tests, the seal was operated with an open-loop control system. These tests demonstrate that a significant variation in leakage rate (and film thickness) can be obtained with the controllable seal.

In the present study, the above electronically controlled seal has been integrated with a closed-loop control system, and examined while being subjected to various operating transients (6). These transients include ramp, step, and oscillating changes in the sealed pressure and operating speed. The feedback to the control system is either the leakage rate or temperature of the nonrotating seal face.

PRINCIPLE OF OPERATION AND SEAL CONFIGURATION

In a conventional mechanical seal, the film thickness is determined by the location of the floating seal face, which is determined by the forces acting upon it. The sealed pressures acting on the backside of the face and the spring produce a closing force, which tends to close the gap between the faces. Opposing the closing force is an opening force, which is produced by the pressure distribution in the lubricating film. One could therefore control the film thickness by controlling either the closing force (4) or the opening force (1-3). In the present work, it is the opening force that is controlled.

To regulate the opening force, it is necessary to control the pressure distribution in the lubricating film. The pressure distribution is strongly influenced by the geometry of the surfaces

of the seal faces. In a conventional seal, the faces are not parallel but converge in the radial direction. This convergence is known as coning and is defined by,

$$\delta = h_o - h_i \tag{1}$$

In a hydrostatic seal, the opening force increases as the nondimensional coning increases (6), the latter being defined by,

$$\delta^* = \delta / h_i \tag{2}$$

For steady state operation, the closing and opening forces are equal; therefore, specifying the closing force determines δ^*, which then remains constant. Thus, the film thickness (h_i) will be proportional to the coning (δ): the larger the coning the larger the film thickness. In the electronically controlled seal, the film thickness is controlled by controlling the coning.

The electronically controlled seal is presented in Figure 1. The double seal configuration consists of two stators and a rotor. The stators are the floating components of the seal; each consists of a deformable face assembly, a holder, six coil springs and two o-rings. Each deformable face assembly consists of a piezoelectric element bonded to a carbon face, a thermocouple embedded in the carbon, electrodes, and wires to the electrodes. The electrodes for the piezoelectric element are located on the axial surfaces of the element. The carbon face is utilized as the ground electrode while the high voltage electrode is on the opposite surface. Since the poling axis for the piezoelectric element is in the radial direction, this configuration produces a shear deformation of the piezoelectric element when a voltage is applied to the

electrodes. The attached carbon face then deforms to produce coning.

TEST SETUP

The intent of the seal tests is to demonstrate the feasibility of an electronically controlled seal for use in the helium purge assembly of a liquid oxygen turbopump. Therefore, the seal is designed to fit in a sealing envelope representative of the size found in such turbopumps, and to operate at relatively high speeds (3770 rad/sec). The dimensions of the sealing envelope for the test rig are presented in Figure 2. The actual temperatures that occur in a liquid oxygen turbopump are not simulated.

Figure 3 presents a schematic of the test setup, which consists of the electronically controlled seal (shown in Figure 1), the seal tester, the motor and belt drive system, the gas supply system, and the instrumentation. The holder for the electronically controlled seal is fabricated from boron nitride, which is electrically insulating yet thermally conductive. PZT-5H (a grade of lead zirconate titanate) is used for the piezoelectric element. The carbon for the nonrotating face is a resin impregnated carbon. The rotor is fabricated from tungsten carbide.

The seal tester consists of the housing, the shaft, and the bearings for the shaft. The housing is constructed from aluminum while the shaft is constructed from O-1 tool steel. The bearings are high speed, deep-groove ball bearings. The seal tester is driven by a belt-drive system that

is powered by a one-horsepower universal motor. The seal is operated with compressed air, which is supplied to the seal tester through copper tubing.

The instrumentation for the test setup consists of a high voltage power supply to drive the piezoelectric actuator, thermocouples and thermocouple readers, an electronic flowmeter located in the air supply line, an electronic pressure transducer (also located in the air supply line) and a tachometer attached to the motor. These instruments are integrated with a microcomputer-based data acquisition system. The closed-loop control system is based on a proportional, integral, derivative (P.I.D.) control algorithm that is defined by,

$$O(t) = K_P e(t) + K_I \int_0^t e(\tau)\, d\tau + K_D \frac{de(t)}{dt} \qquad (3)$$

The feedback to the control system is either the leakage rate of the seal, which is measured by an electronic flowmeter in the gas supply line, or the temperature of the carbon face, which is measured by a thermocouple. The output of the control system is the voltage applied to the deformable face assembly.

Additional instrumentation is necessary to measure the coning of the carbon faces (while they are removed from the seal tester): an optical flat and a monochromatic light source with a wavelength of 0.546 μm.

RESULTS

Since active control of the film thickness is established through the action of the deformable face assembly, it is useful to examine the coning deformation of the carbon face versus the voltage applied to the piezoelectric actuator. Figure 4 presents the coning deformation, measured with the face assembly removed from the test rig housing. Therefore, these results omit the deformations due to pressure and thermal loading. The carbon face used for this test has an outside diameter of 34.80 mm, and an inside diameter of 24.00 mm.

One of the curves presented in Figure 4 shows the coning deformation for a voltage loading that begins at 3000 V, decreases in 500 V steps to -3000 V, and then increases in 500 V steps back to 3000 V. It demonstrates that a range of coning from approximately 2 to -3.5 μm is produced by the deformable face assembly.

The coning deformation exhibits a significant amount of hysteresis. The decreasing portion of the voltage loading path from 3000 V to -3000 V exhibits a larger positive coning than over the increasing portion of the voltage loading from -3000 V to 3000 V. At 0 V there is a difference of 3 μm between the increasing and decreasing portions of the voltage loading curve.

Figure 4 also presents the coning deformation over a voltage range from 3000 to 0 V. Over this reduced voltage range, the range of coning is reduced and varies from 2.2 to 0.5 μm. The hysteresis in the coning is also reduced. Voltage levels for the transient testing (described

below) are typically limited to this reduced voltage range.

Short term transient tests of the seal, utilizing either the leakage rate or face temperature as the feedback signal, have been performed. For the tests in which leakage rate is used as the feedback signal, the constants for the P.I.D. controller are set as follows: K_P = 0.1 V/slm, K_I = 0.2 V/(slm sec), and K_D = 0.01 (V sec)/slm. For the tests in which face temperature is used as the feedback signal, the P.I.D. constants are K_P = -0.5 V/C, K_I = -0.1 V/C sec), and K_D = -0.5 (V sec)/C.

Figure 5 presents the speed and pressure transients that are imposed on the seal for these tests. The seal is operated for approximately three minutes with a cavity pressure of 1.48 x 10^6 Pa, and a rotational speed of 3770 rad/sec. A ramp decrease in speed to 2000 rad/sec then occurs, followed by a ramp increase to 3770 rad/sec. This is followed by a step decrease in speed to 2000 rad/sec, followed by a step increase to 3770 rad/sec. After the speed transients, the pressure transients are imposed in a similar manner. During the pressure transients, the pressure varies from 1.48 x 10^6 Pa to 4.46 x 10^5 Pa.

Figure 6 presents the leakage rate and face temperature versus time for the test that utilizes the leakage rate as the feedback signal, with a set point leakage rate of 12 slm. Figure 6 demonstrates that the leakage rate is maintained close to the set point during the entire test. The temperature varies but remains below 85 C, which is well within the temperature limits of the seal components.

The largest deviations in the leakage rate from the set point occur during the stepwise pressure transients. However, this does not represent a serious problem because the deviation occurs for a very short duration of time, and therefore does not represent a significant increase in air leakage. Furthermore, the face temperature does not increase significantly, thereby indicating that extended face contact does not occur.

Figure 7 presents the voltage applied to the piezoelectric element versus time for the above test. This figure demonstrates that the control system is very active: the full voltage range of 0 to 3000 V is utilized. As the speed is decreased, the voltage generally increases. This can be explained by considering the thermally induced coning. As the speed decreases, the viscous heat generation produced between the seal faces is reduced. This in turn decreases the temperature of the seal faces. Previous analyses [Wolff, 1993] demonstrate that the thermally induced coning decreases as the face temperatures decreases. Therefore, the voltage must increase as the temperature decreases, to maintain the set point leakage rate.

Hydrodynamic effects could also partially account for the increase in voltage as the speed is reduced. Slight misalignment between the seal faces could cause the leakage rate to be speed dependent. Then, as the speed decreases, an increase in voltage is necessary to maintain the set point leakage rate.

Figure 8 presents the leakage rate and face temperature versus time, for the short term test in which the face temperature is used as the feedback signal. The transients imposed are the same

as the ones for the aforementioned test (Figure 5). The face temperature is maintained close to the set point of 80 C during this test, with maximum deviations of approximately 3 C occurring during the stepwise pressure transients. The leakage rate varies from 2 to 16 slm.

The wide variation in leakage rate points out a disadvantage of utilizing the face temperature as the feedback signal. The large reductions in leakage rate are undesireable, since they increase the risk of face contact. It is therefore believed that the previous control scheme, i.e., that in which the leakage rate is controlled, is superior.

Figure 9 presents the voltage and speed versus time for the above test. The voltage decreases as the speed is decreased, which is opposite to what occurs during the test in which leakage rate is used as the feedback signal. Again, this can be explained by considering the viscous heat generation between the seal faces. As the speed decreases, the viscous heat generation also decreases. Therefore the voltage must be reduced to decrease the film thickness, in order to maintain the same viscous heat generation rate, which prevents the face temperature from decreasing.

Longer term transient tests have also been conducted. These consist of a series of thirty-minute cycles over a period of approximately four hours. Figure 10 shows a typical operating cycle, which consists of a startup and shutdown, as well as speed and pressure transients. The speed and pressure transients include step changes in speed and pressure, and oscillating variations in speed and pressure. The oscillating variation is a harsher transient than the ramp changes (in

the short term tests); therefore, the latter are not included in the long term transient tests.

The leakage rate is utilized as the feedback signal for the long term transient tests, since the short term tests demonstrate the disadvantages of utilizing the face temperature as the feedback signal for the P.I.D. controller. For the long term tests, the constants for the P.I.D. controller are $K_P = 0.3$ V/slm, $K_I = 0.2$ V/(slm sec), and $K_D = 0$ (V sec)/slm. The set point leakage rate is 12 slm.

Figure 11 presents the leakage rate and face temperature for one of the long term tests. This figure demonstrates that the seal can operate successfully for an extended period of time. The leakage rate is maintained near the set point of 12 slm while the face temperature remains below 85 C. (The large drop in temperature at 120 min. is due to a test interruption.) The largest deviations in the leakage rate from the set point occur during the oscillating pressure transients. However, these deviations do not pose a serious problem because they last for only a brief period of time, and the face temperature does not increase significantly.

An additional long term test has been performed, in which the voltage level is held constant at 2000 V to ensure that the faces are coned in the positive direction, thus promoting the existence of a lubricating film between the seal faces. During startup however, the voltage is increased to a higher level to reduce the startup torque. The transient operating conditions imposed during this test are similar to those presented in Figure 10.

Figure 12 presents the leakage rate and face temperature for this test. The leakage rate and face temperature fluctuations are larger than those in Figure 11. However, over this four hour test, the leakage rate is generally maintained at a level less than 10 slm, and the face temperature never exceeds 90 C. Thus, a very simple control strategy would be to maintain a constant voltage level high enough to maintain a lubricating film between the seal faces. During startup and shutdown transients, an increase in the voltage level would sustain the lubricating film.

Figure 13 presents the results from a test that simulates the operation of a conventional seal. The voltage for this test is maintained at 0 V, thus simulating the operation of an uncontrolled seal. The operating transients are identical to those presented in Figure 10.

Figure 13 demonstrates that the seal performs poorly without the control system. During the first cycle of operation, the face temperature reaches approximately 110 C. During the second cycle, the face temperature increases dramatically to approximately 120 C after the step increase in pressure. The test must then be aborted to prevent damage to the seal components. Comparison of Figure 13 with Figure 11 (or 12) dramatically illustrates the superiority of the electronically controlled seal.

CONCLUSIONS

The results from this study indicate that an electronically controlled seal for aerospace

applications is feasible. The seal has been operated for short term and longer term tests with a closed-loop control system while being subjected to speed and pressure transients. The control system is capable of utilizing either the leakage rate or the face temperature as the feedback signal. Low leakage rates and face temperatures have been maintained, thus demonstrating successful operation of the seal.

ACKNOWLEDGMENTS

This work has been supported by the National Aeronautics and Space Administration, Lewis Research Center, under Grant NAG 3-974. The NASA Technical Officer has been M. P. Proctor. The authors wish to acknowledge the Pure Carbon Company, who supplied the carbon graphite seal faces, and Mr. Samuel Navon, who made important contributions to the seal design.

REFERENCES

1. Salant, R.F., Miller, A.L., Kay, P.L., Kozlowski, J., Key, W.E. and Algrain, M.C., "Development of an Electronically Controlled Mechanical Seal," in *Proc. 11th Intl. Conf. Fluid Sealing*, Nau, B.S., ed., BHRA, Cranfield, UK (1987), pp. 576-595.

2. Heilala A.J. and Kangasniemi, A., "Adjustment and Control of a Mechanical Seal Against Dry Running and Severe Wear," in *Proc. 11th Intl. Conf. Fluid Sealing*, Nau, B.S., ed., BHRA, Cranfield, UK (1987), pp. 548-575.

3. Salant R.F., Giles O. and Key, W.E., "Design of Controllable Mechanical Seals," in *Tribological Design of Machine Elements*, Dowson, D., ed., Elsevier, Amsterdam, The Netherlands (1989), pp. 47-55.

4. Etsion I., Palmor Z. and Harari N., "Feasibility Study of a Controlled Mechanical Seal," *Lubr. Eng.*, **47**, 8, pp. 621-625 (1991).

5. Salant, R.F., Wolff, P.J. and Navon, S., "Electronically Controlled Mechanical Seal for Aerospace Applications - Part I: Design, Analysis and Steady State Tests," *Tribology Transactions*, **37**, 1 (1994).

6. Wolff, P.J., "Experimental Investigation of an Actively Controlled Mechanical Seal," Georgia Institute of Technology, Atlanta, Ga., Ph.D. Thesis (1993).

LIST OF FIGURES

fig. 1

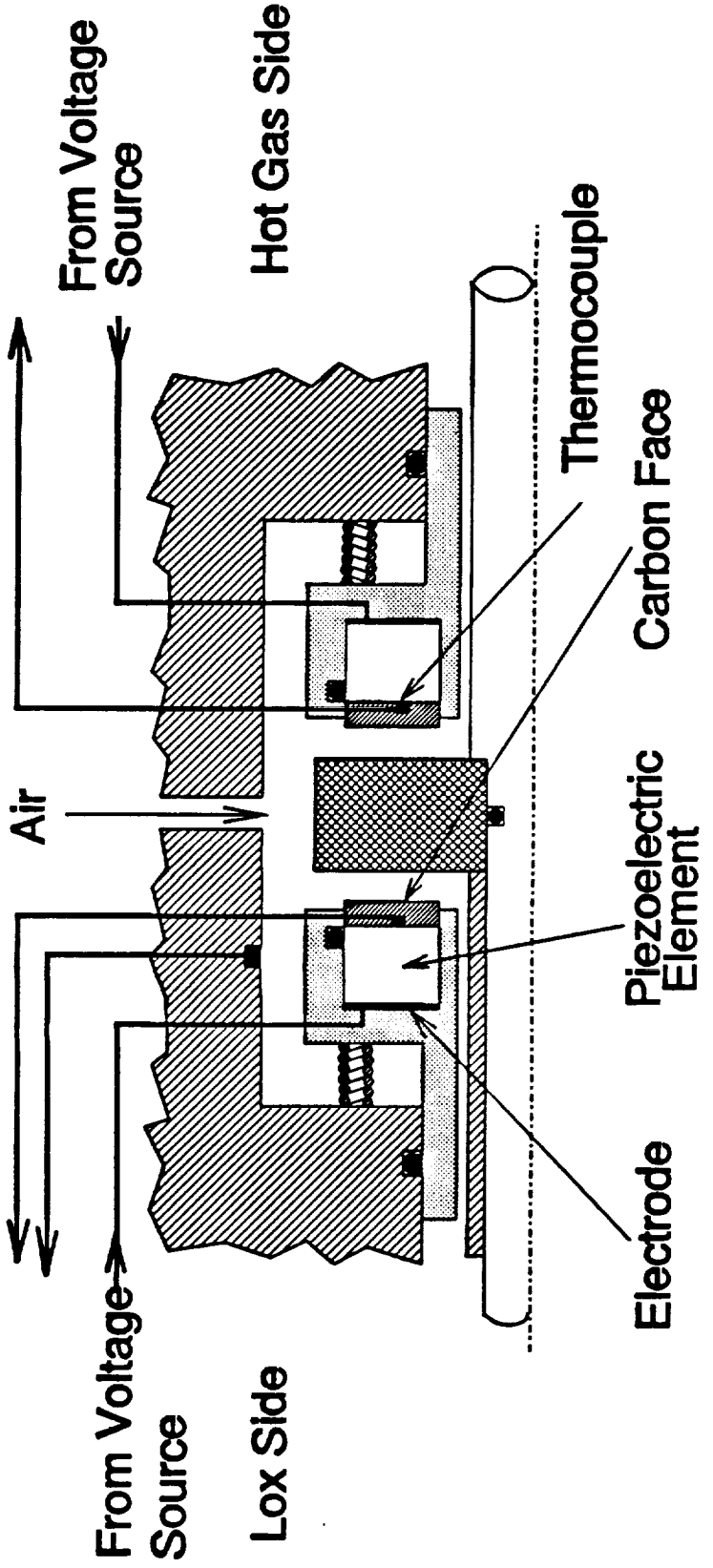
From Voltage Source
Hot Gas Side
Thermocouple
Carbon Face
Air
Piezoelectric Element
Electrode
From Voltage Source
Lox Side

fig. 2

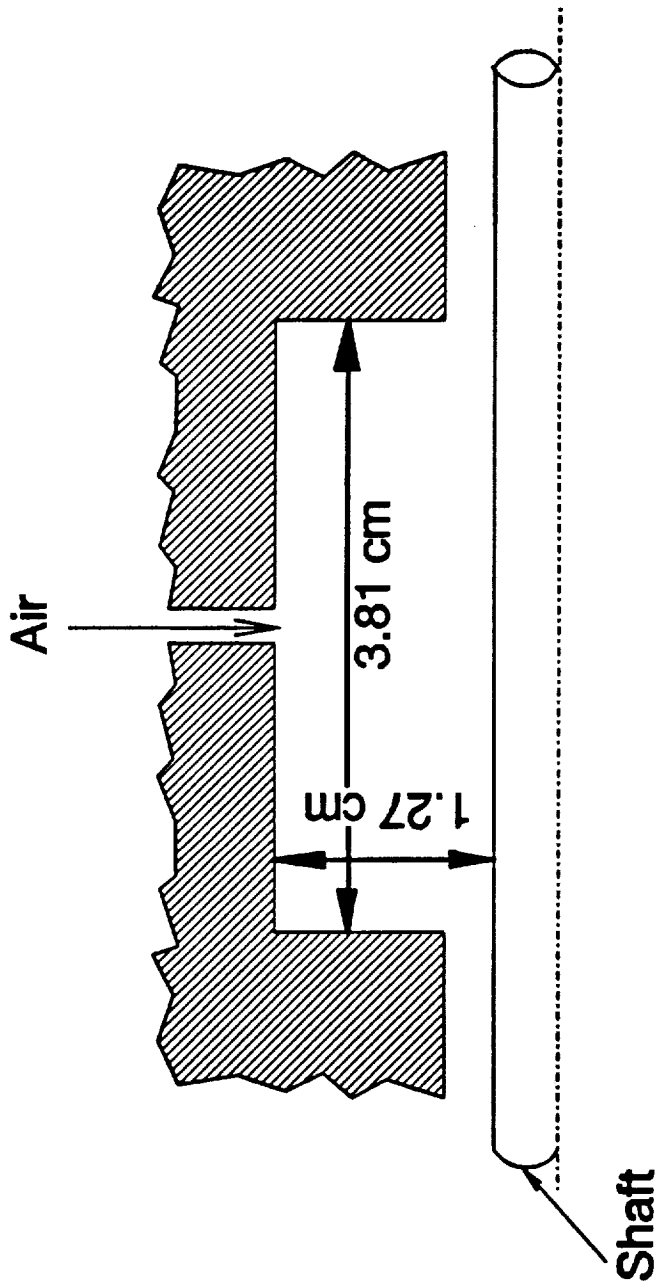

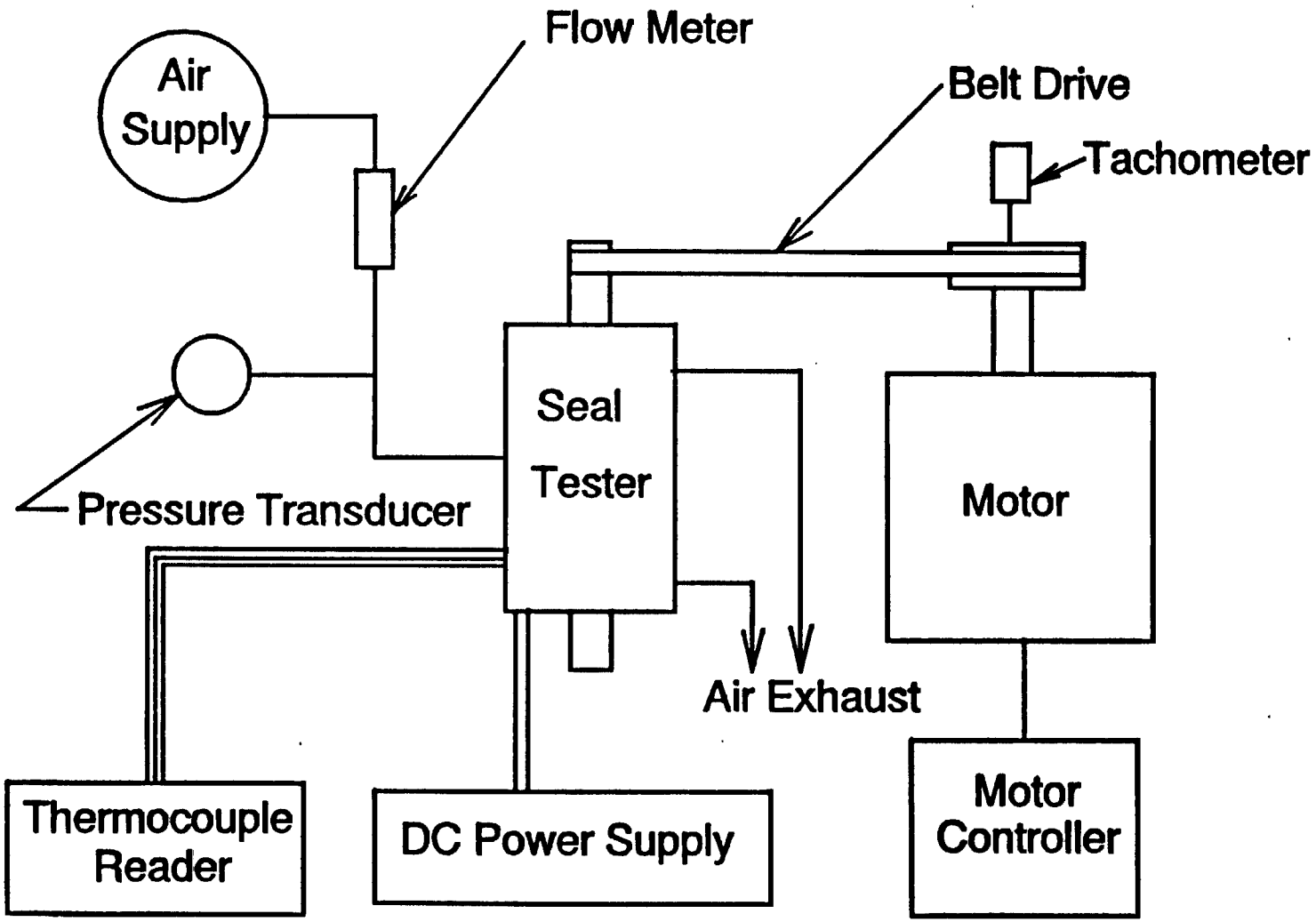
Air Supply
Flow Meter
Belt Drive
Tachometer
Pressure Transducer
Seal Tester
Motor
Air Exhaust
Thermocouple Reader
DC Power Supply
Motor Controller

Fig. 3

fig. 4

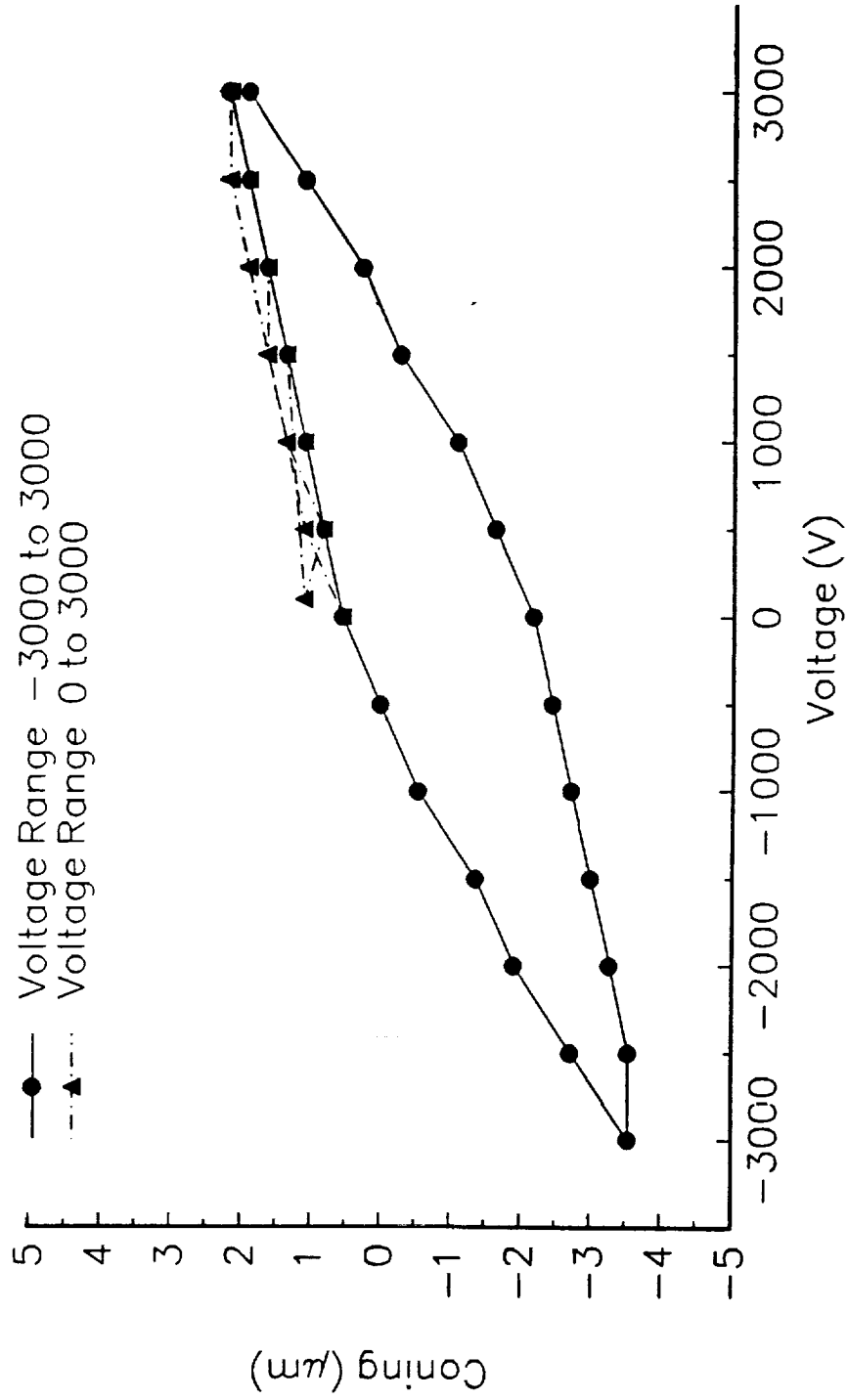
Voltage Range −3000 to 3000
Voltage Range 0 to 3000
Coning (μm)
5
4
3
2
1
0
−1
−2
−3
−4
−5
−3000
−2000
−1000
0
1000
2000
3000
Voltage (V)

Fig. 5

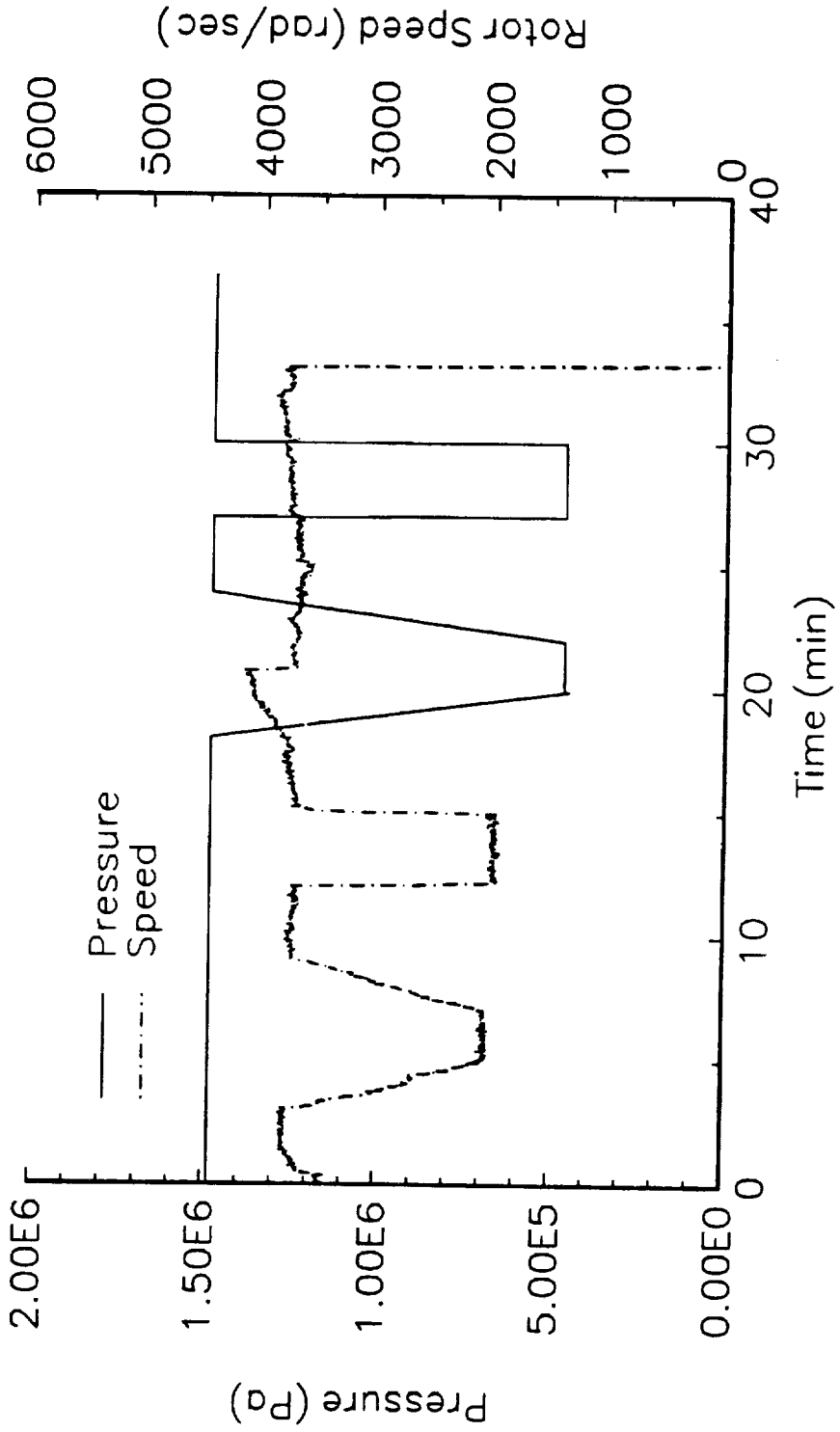
Rotor Speed (rad/sec)
6000
5000
4000
3000
2000
1000
0
40
30
20
10
0
Time (min)
Pressure
Speed
2.00E6
1.50E6
1.00E6
5.00E5
0.00E0
Pressure (Pa)

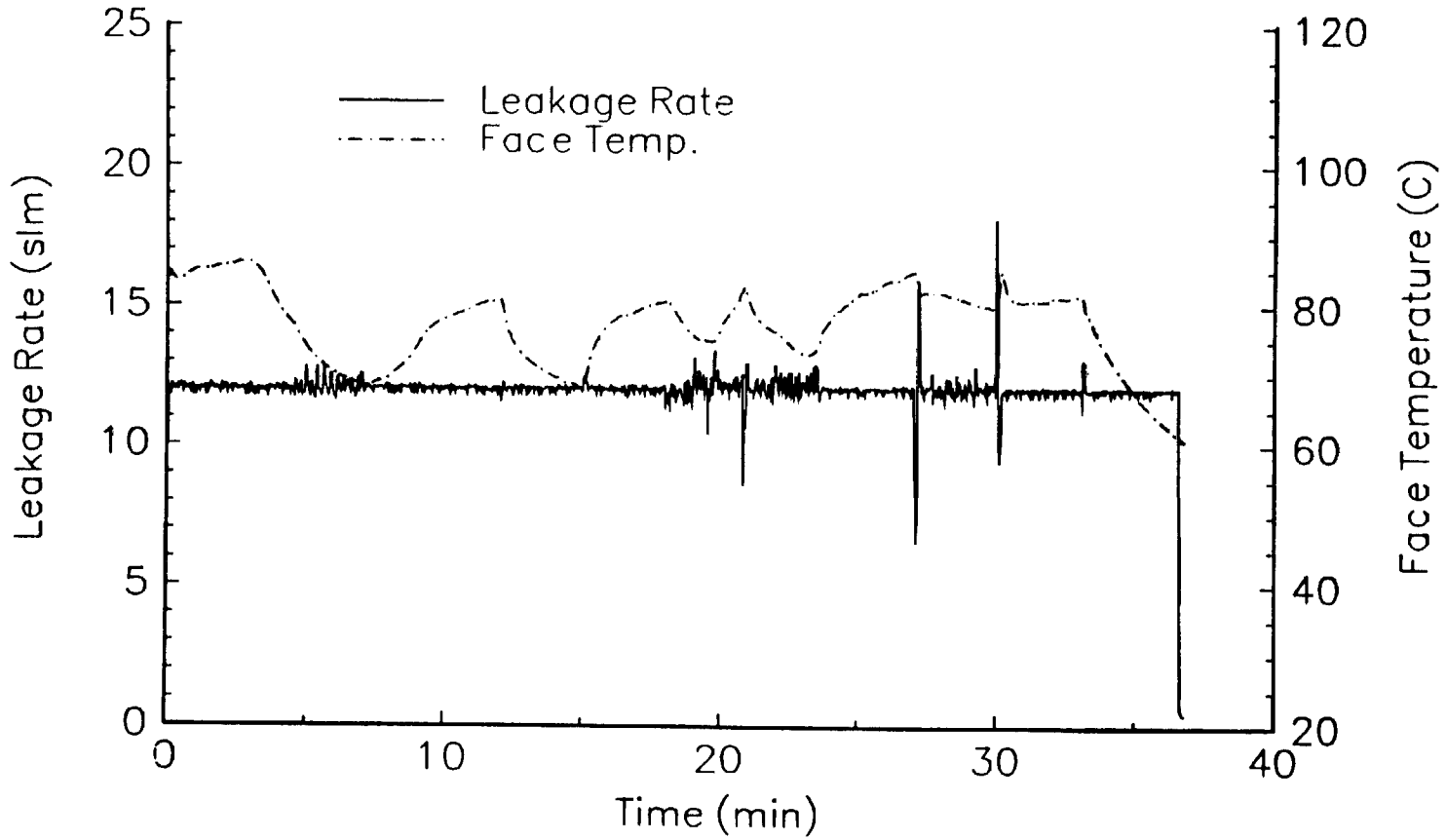
Leakage Rate
Face Temp.
Leakage Rate (slm)
Face Temperature (C)
Time (min)
0
5
10
15
20
25
20
40
60
80
100
120
0
10
20
30
40

Fig. 6

Fig. 7

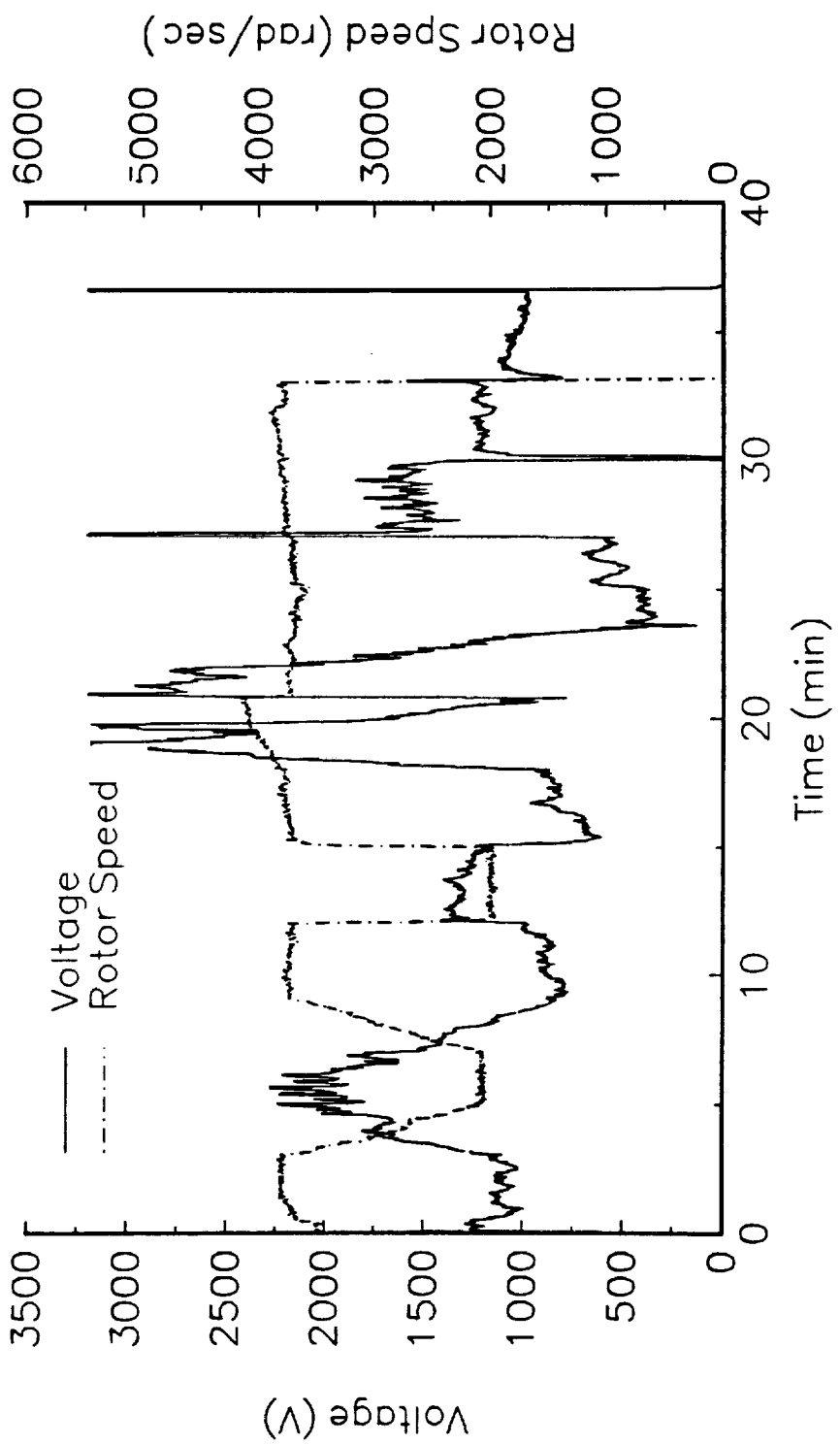
Voltage (V)
Rotor Speed (rad/sec)
Time (min)
Voltage
Rotor Speed
3500
3000
2500
2000
1500
1000
500
0
6000
5000
4000
3000
2000
1000
0
0
10
20
30
40

Leakage Rate (slm)
25
20
15
10
5
0
Face Temp. (C)
120
100
80
60
40
20
0
10
20
30
40
Time (min)
Leakage
Face Temp.

Fig. 8

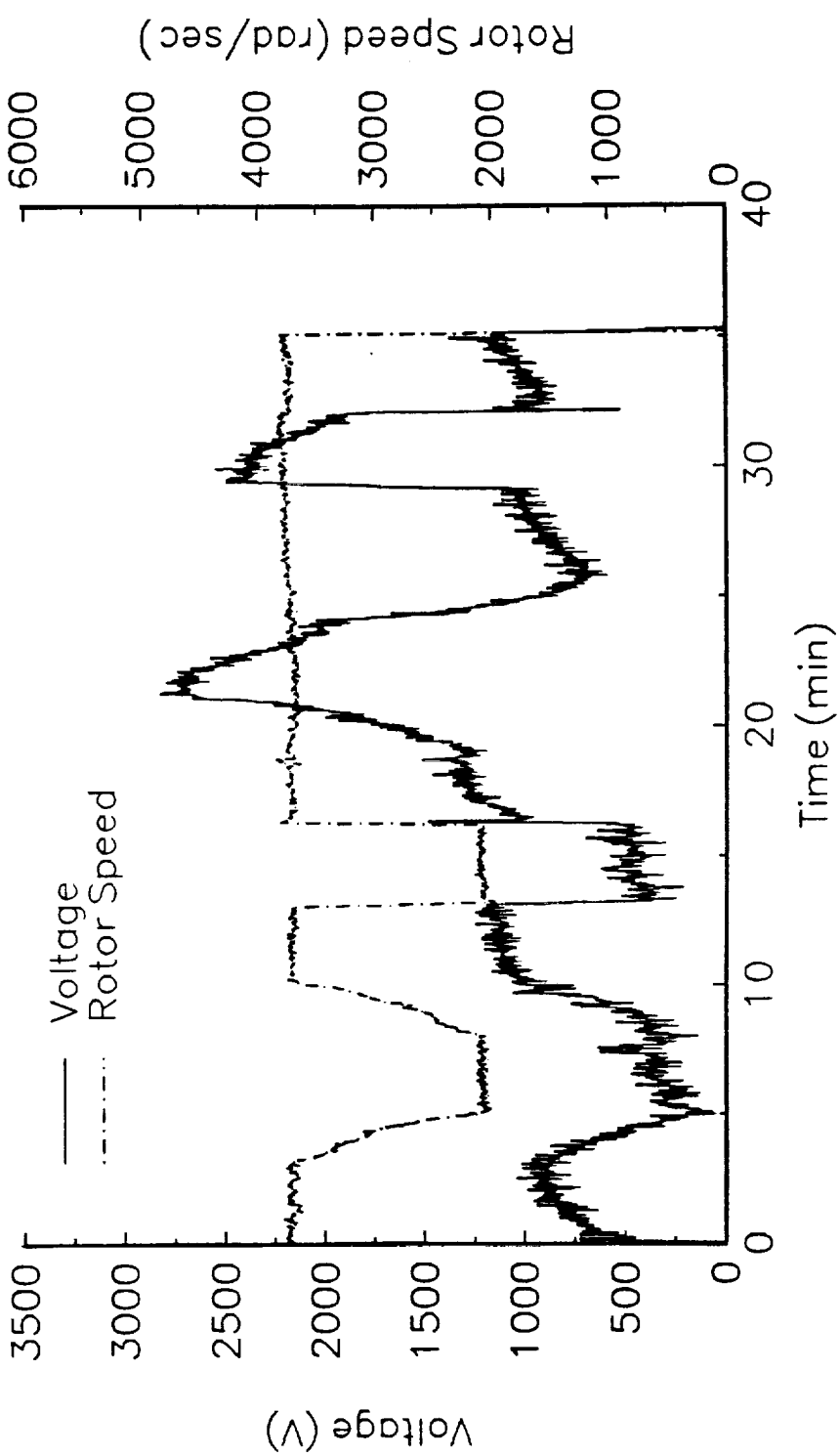
Voltage (V)
3500
3000
2500
2000
1500
1000
500
0
Rotor Speed (rad/sec)
6000
5000
4000
3000
2000
1000
0
Time (min)
0
10
20
30
40
Voltage
Rotor Speed

fig. 9

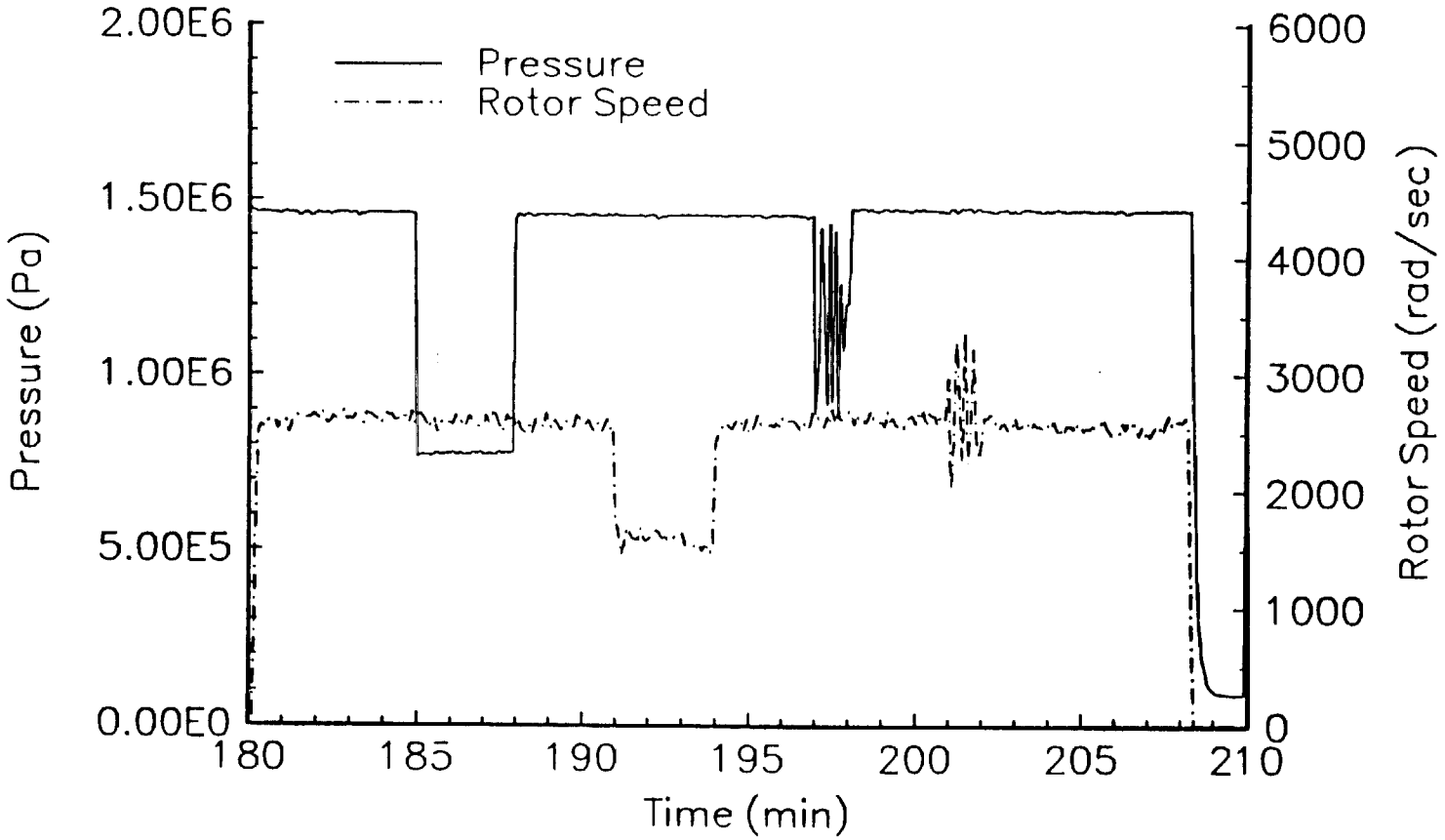
Pressure
Rotor Speed
2.00E6
1.50E6
1.00E6
5.00E5
0.00E0
Pressure (Pa)
6000
5000
4000
3000
2000
1000
0
Rotor Speed (rad/sec)
180
185
190
195
200
205
210
Time (min)

Fig. 10

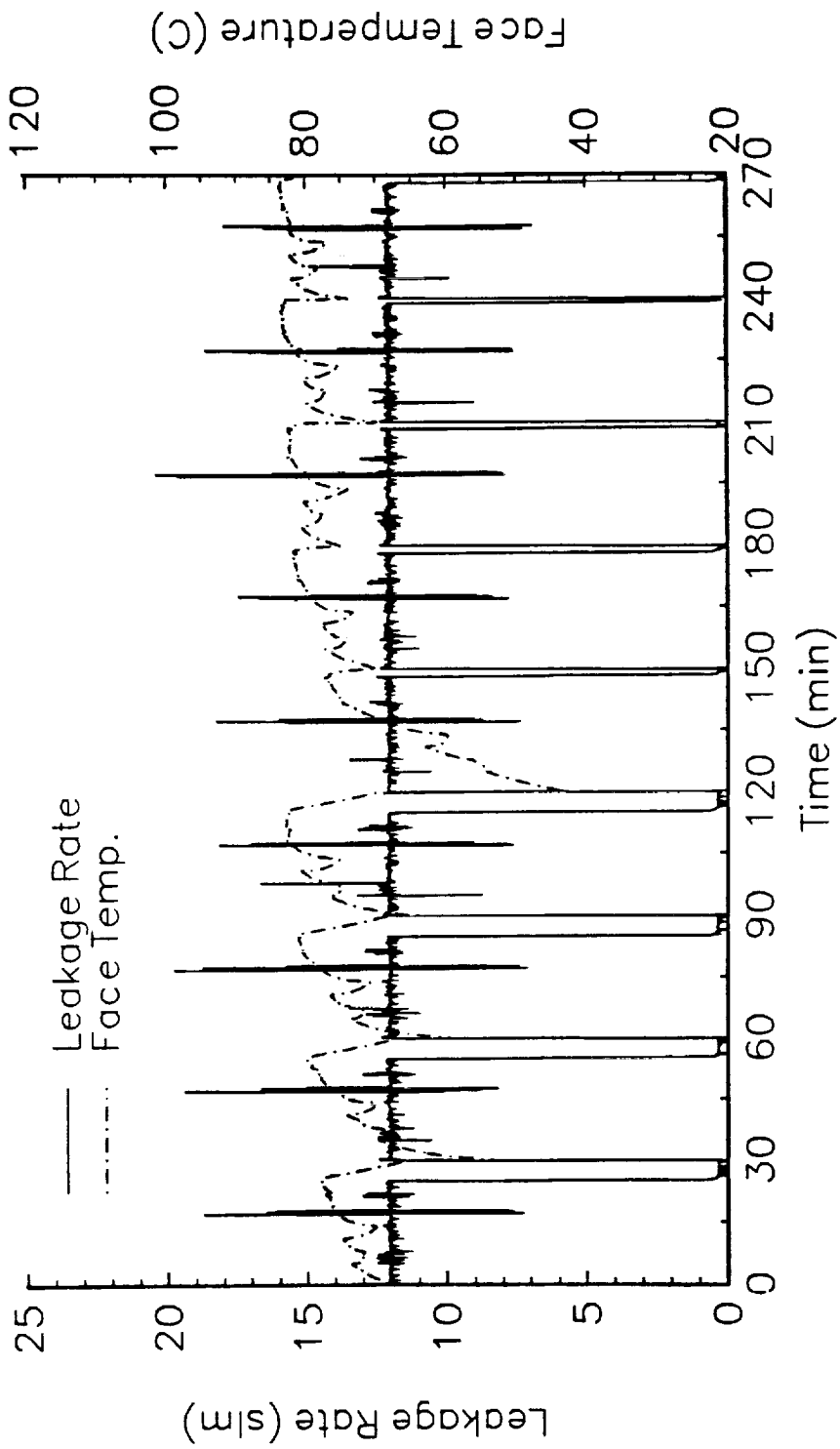
Face Temperature (C)
120
100
80
60
40
20
Leakage Rate (slm)
25
20
15
10
5
0
Leakage Rate
Face Temp.
0
30
60
90
120
150
180
210
240
270
Time (min)

fig. 11

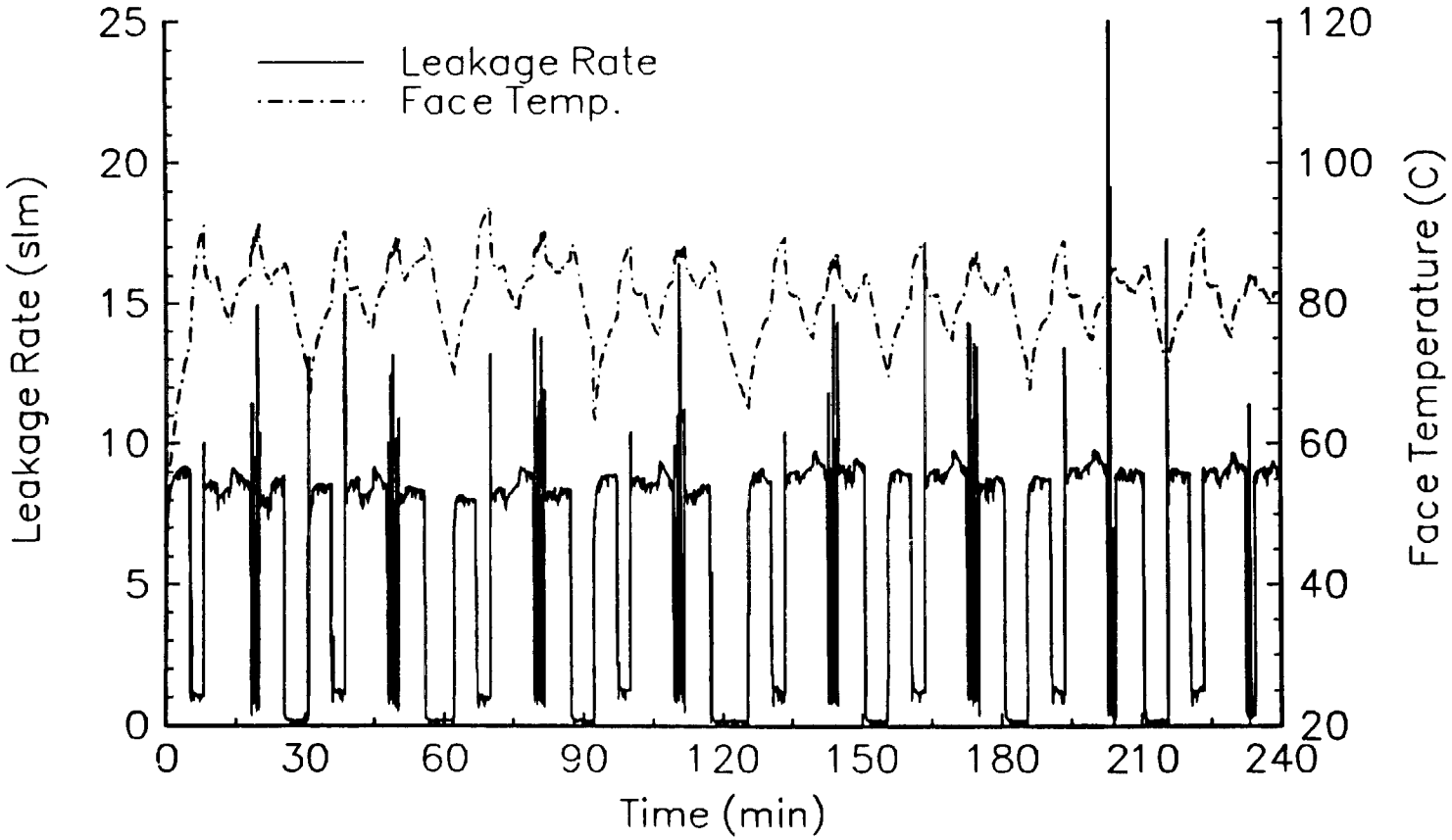
Leakage Rate
Face Temp.
Leakage Rate (slm)
Face Temperature (C)
Time (min)
0
5
10
15
20
25
20
40
60
80
100
120
0
30
60
90
120
150
180
210
240

Fig. 12

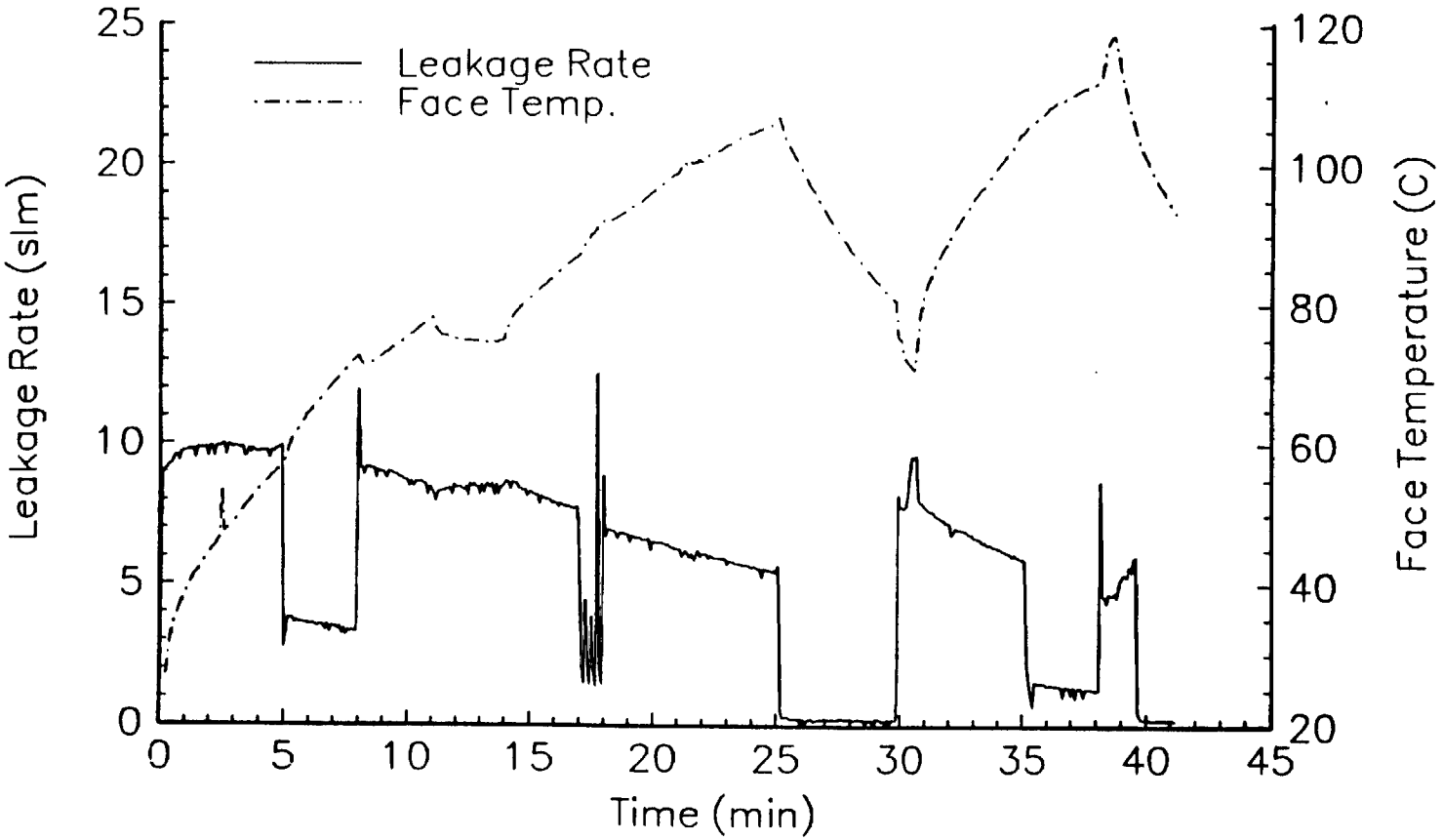
Leakage Rate
Face Temp.
Leakage Rate (slm)
Face Temperature (C)
Time (min)
0
5
10
15
20
25
30
35
40
45
0
5
10
15
20
25
20
40
60
80
100
120

Fig. 13

DEVELOPMENT OF AN ELECTRONICALLY CONTROLLED MECHANICAL SEAL FOR AEROSPACE APPLICATIONS

Richard F. Salant, Georgia Institute of Technology
Paul J. Wolff, Tennessee Valley Authority

ABSTRACT

An electronically controlled mechanical seal, in a configuration suitable for aerospace applications, has been built and tested in the laboratory. The thickness of the lubricating film between the seal faces is controlled by adjusting the coning of one of the faces, which is bonded to a piezoelectric crystal. An applied voltage causes the crystal to deform in the shear mode, thereby inducing coning of the seal face; the larger the voltage, the larger the coning. The coning affects the fluid mechanics of the film such that the larger the coning, the larger the average film thickness. Therefore the film thickness increases with increased applied voltage.

Steady state tests have shown that the leakage rate (and therefore, the film thickness) can be adjusted over a substantial range, utilizing the available range of voltage. Transient tests have shown that either the leakage rate or the face temperature can be maintained near a set point during both gradual and abrupt changes in operating conditions, by utilizing a closed-loop control system.

INTRODUCTION

In most aerospace applications requiring rotating shaft seals, fixed clearance seals (e.g., floating ring seals, bushings, labyrinth seals) are used. Such seals have the advantage that the mating surfaces in relative motion can never be in mechanical contact. Thus, the probability of seal failure or excessive wear is very low. The disadvantage of such seals is their high leakage rate, relative to other types of seals. This is a consequence of the relatively large clearance between the mating surfaces, resulting from the need to accommodate manufacturing tolerances (e.g., shaft misalignment).

An alternative to the fixed clearance seal is the noncontacting mechanical (face) seal, shown schematically in figure 1. In the latter seal, one of the faces floats in the axial direction and dynamically tracks the mating face, maintaining a continuous fluid film between the faces. Since this seal is self-adjusting and self-aligning, it can operate with a much smaller clearance between the mating surfaces (film thickness) than the fixed clearance seal. Typically, the film thickness in a noncontacting mechanical seal is one-tenth that of the film

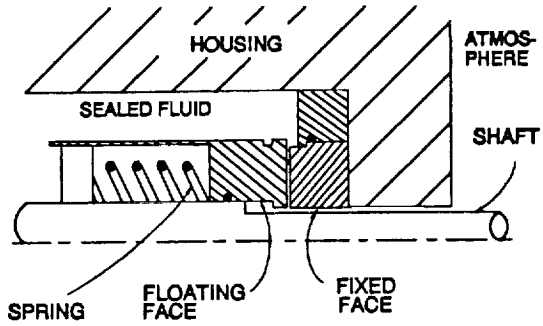

Figure 1 Schematic of mechanical seal.

thickness in a fixed clearance seal. Since the leakage rate is approximately proportional to the cube of the film thickness, noncontacting mechanical seals will have leakage rates on the order of one-thousandth those of fixed clearance seals. This low leakage rate is one of the principal advantages of the mechanical seal.

The principal disadvantage of the noncontacting mechanical seal is related to the possibility that the two mating faces can come into mechanical contact while in relative motion. Such seals are designed so that a continuous fluid film separates the two faces at the design point. However, if transients occur or steady state operating conditions change, the film thickness will change and it is possible that mechanical contact will occur. Sustained mechanical contact produces mechanical and thermal damage to the faces, leading to excessive wear and reduced reliability. Therefore in aerospace applications, where high reliability and low wear are important requirements, fixed clearance seals are generally preferred.

In recent years, however, a number of researchers have combined the high reliability and low wear rate of the fixed clearance seal with the low leakage rate of the mechanical seal, by developing a controllable mechanical seal, viz., a mechanical seal whose film thickness can be controlled (1-4). With such a seal, if operating conditions change such that face contact is imminent, the film thickness can be adjusted to a larger value and face contact minimized or avoided. Conversely, if operating conditions change such that leakage

is excessive, the film thickness can be adjusted to a lower value, to maintain the leakage rate at an acceptable level.

Since the film thickness is determined by the axial location of the floating face, and since that location is determined by the forces acting on the floating face, control of the film thickness can be achieved through control of the appropriate forces. Two types of forces act on the floating face. The closing force that tends to close the gap between the faces is produced by the spring and sealed pressure acting on the backside of the floating face. The opening force that tends to open the gap is produced by the pressure distribution in the fluid film. Under equilibrium conditions, the floating face will assume an axial position such that the closing forces are balanced by the opening forces. Thus, one could control the film thickness by controlling either the closing force (4) or the opening force (1-3). In the present work, the latter approach is used.

It would appear that a controllable mechanical seal would be a viable low-leakage alternative to the fixed clearance seal in some aerospace applications. However, it should be noted that the previous work on controllable mechanical seals has been directed toward industrial applications, where constraints on size and weight are not as stringent as in aerospace applications. The object of the present work, therefore, is to demonstrate the feasibility of a controllable mechanical seal in a typical aerospace application.

DEMONSTRATION APPLICATION

The representative aerospace application chosen for the present study is the purge gas seal assembly of a liquid oxygen turbopump. A typical conventional assembly is shown in figure 2. A pressurized purge gas, such as helium, is

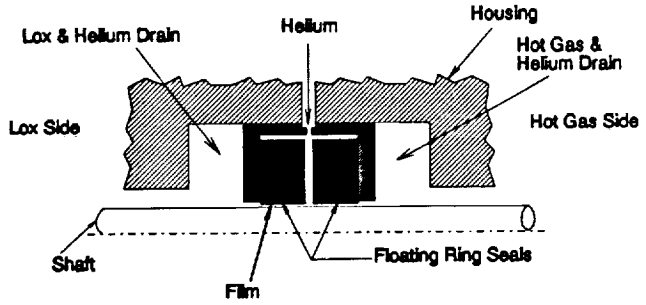

Figure 2 Conventional purge gas seal assembly (5).

introduced near the midpoint of the turbopump, in order to prevent the hot gases on the turbine side of the turbopump from contacting the oxygen on the pump side. The purge gas leaks through two floating ring seals. The leakage towards the turbine side mixes with the turbine gases and is removed through a drain; the leakage towards the pump side mixes with the oxygen and is removed through a second drain. The dimensions of the assembly envelope are 38.1 mm (1.50 in) in the axial direction and 12.7 mm (0.50 in) in the radial direction from the outside radius of the shaft to the outside radius of the envelope.

It is proposed to replace the floating ring seals in the above assembly with electronically controlled mechanical seals.

PRINCIPLE OF OPERATION

To control the film thickness in a mechanical seal, it is necessary to control either the opening force or the closing force. In the present study, the opening force (which is produced by the pressure distribution in the film) is controlled.

It should be noted that under normal operating conditions, the sealing surfaces of the faces in a mechanical seal are not perfectly parallel, but are slightly coned, as shown in figure 3. The coning, δ, is defined as the difference between the film

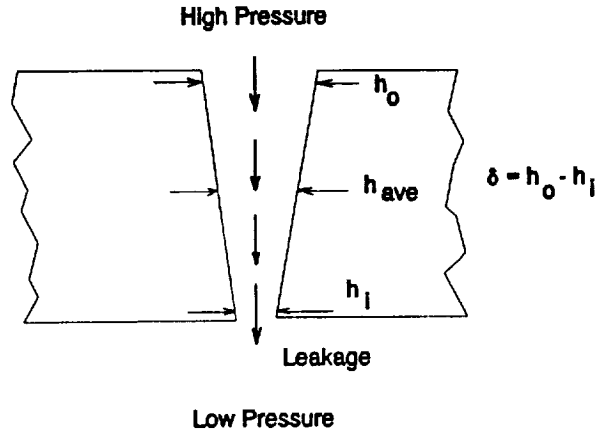

Figure 3 Coned seal faces.

thicknesses at the outer radius (h_o) and inner radius (h_i). In a conventional seal this coning is produced by a combination of mechanical and thermal deformation of the seal faces and supporting structure.

The pressure distribution in the film is affected by the above coning. This can be seen from figure 4, which has been obtained by solving the compressible Reynolds Equation for a seal with a radius ratio of 1.45 (6). Note that the pressure

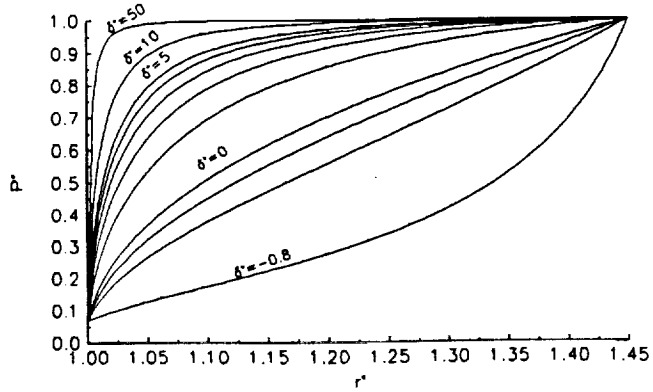

Figure 4 Pressure distribution in film.

distribution, normalized with respect to the sealed pressure, depends on the normalized coning δ^*, where $\delta^* = \delta/h_i$. For seals with positive coning, the larger the δ^* the more convex

the profile and the larger the normalized opening force. For a seal of a given design (given balance ratio), the normalized closing force is fixed. Since the opening force must equal the closing force, the normalized closing force is also fixed and corresponds to some constant value of δ^*, viz., δ/h_i = constant, or $h_i \sim \delta$. Thus, it is seen that the film thickness is proportional to the coning.

The latter relation provides a means of controlling the film thickness. By adjusting the coning, one can adjust the film thickness, since the larger the coning, the thicker the film.

CONFIGURATION OF ELECTRONICALLY CONTROLLED MECHANICAL SEAL

An electronically controlled mechanical seal assembly, to replace the conventional purge gas seal assembly of figure 2, has been designed and built. It is shown schematically in figure 5. A single tungsten carbide rotating face is fixed to the

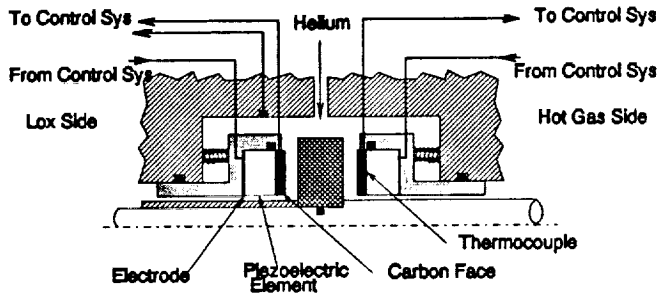

Figure 5 Schematic of electronically controlled seal (5).

shaft. Two non-rotating controllable face assemblies float in the axial direction. Each of the latter assemblies consists of a carbon graphite face bonded to a PZT-5H piezoelectric crystal (in the form of a ring), a copper foil electrode, a boron nitride holder, O-ring secondary seals, and coil springs, as shown. The shaft is supported by two high speed sealed ball bearings (not shown). Leads attached to the copper electrode and the carbon-piezoelectric crystal interface allow a voltage to be placed across the crystal, with the carbon side serving as ground. (Note that the boron nitride used for the holder is an electrical insulator, but a thermal conductor).

The piezoelectric crystal is poled in the radial direction, so that when a voltage is applied across the crystal (in the axial direction), the crystal undergoes shear deformation and causes the carbon face to cone. The larger the applied voltage, the larger the coning and the thicker the fluid film.

To determine how much voltage should be applied to the piezoelectric crystal at any given time, information on the conditions in the film and in the sealed cavity is required. Therefore, a thermocouple is imbedded in each carbon face and a thermocouple is placed near the cavity wall. In addition, an electronic flow meter is used to measure the leakage rate.

APPARATUS

The equipment used to test the seal of figure 5 is shown in figure 6. For ease of testing, compressed air is utilized as the sealed fluid instead of helium. It is supplied to the seal

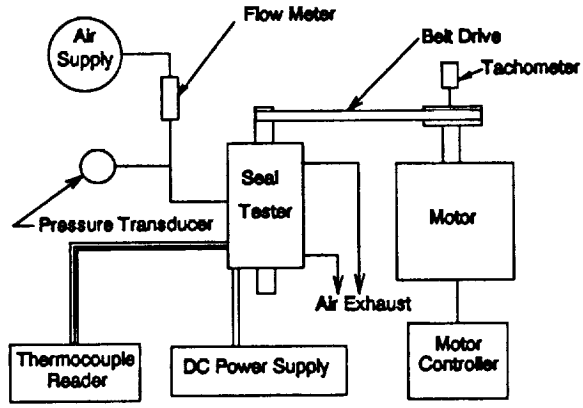

Figure 6 Test Apparatus (5).

tester (containing the seal assembly of figure 5) from a compressed air cylinder. The shaft is driven by a variable speed motor through a belt drive. Voltage is supplied to the piezoelectric crystal from a DC power supply. The principal instrumentation consists of an electronic flow meter and an electronic pressure transducer in the air supply line, a tachometer, and the thermocouples described earlier. The voltage supplied to the piezoelectric crystal can be adjusted manually, or controlled by a microcomputer-based control system (not shown in figure). All instrumentation is integrated into a microcomputer-based data acquisition system.

STEADY STATE TESTS

A series of steady state tests have been performed on the electronically controlled seal to demonstrate that the leakage rate (and, therefore, the film thickness) can be adjusted by adjusting the voltage applied to the piezoelectric crystal. The results of a typical test, with a sealed pressure of 1.34×10^6 Pa (180 psig) at a speed of 3770 rad/sec (36,000 rpm) are

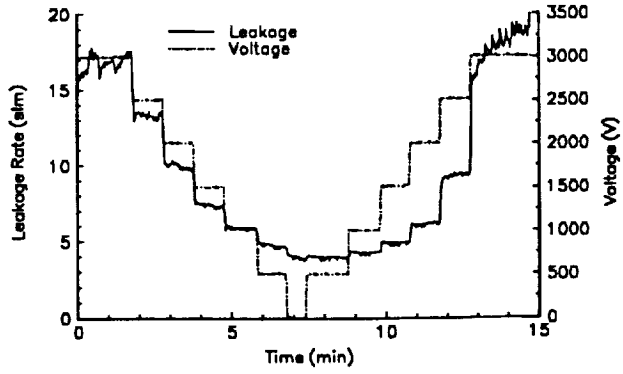

Figure 7 Steady state test results.

shown in figure 7.

In this test 3000 volts is initially applied to the crystal (the

voltage level is set manually). The voltage is then decreased in 500 volt increments to 0 volts, and then increased in 500 volt increments to 3000 volts. The seal is operated at each voltage level for one minute. At each step drop in voltage, there is a corresponding drop in leakage. Over the voltage range of 3000 to 0 volts the leakage rate decreases from 17 to 4 slm (0.60 to 0.14 scfm). Similarly, at each step increase in voltage, there is a corresponding increase in leakage. Over the voltage range of 0 to 3000 volts the leakage rate increases from 4 to 19 slm (0.14 to 0.67 scfm).

These results demonstrate that the leakage rate can be varied over a considerable range, by varying the applied voltage. These results also show hysteresis in the seal response. Over the decreasing portion of the curve, the leakage rate is generally higher than that over the increasing portion of the curve, for the same voltage level. The hysteresis can be more clearly seen in figure 8, which contains a plot of leakage rate (for a single seal, one-half that of the assembly) versus voltage. Also shown on the plot is a predicted leakage

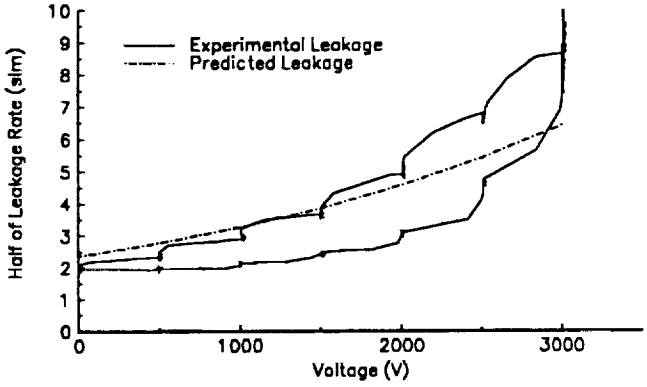

Figure 8 Steady state leakage rate vs. voltage.

curve, obtained from a theoretical analysis (6).

The hysteresis displayed in figure 8 (and in figure 7) arises from two sources. First, bench tests of coning of the piezoelectric crystal have shown that the crystal response itself exhibits hysteresis. Second, it is expected that the movement of the floating seal face will exhibit hysteresis, due to the presence of O-rings. It should be noted, however, that the presence of hysteresis is not expected to have a deleterious effect on performance, since this seal is intended to operate with a closed loop control system, which can compensate for the hysteresis (see next section).

Figure 9 shows the temperature histories of the sealed cavity and of the carbon seal face, during the steady state test of figures 7 and 8. As would be expected, the temperatures of both the cavity and the seal face increase as the leakage rate decreases, and decrease as the leakage rate increases. This is because lower leakage rates correspond to thinner films, in which the viscous heating rate is higher because of higher shear stresses.

TRANSIENT TESTS

In the steady state tests described above, the voltage applied to the piezoelectric crystal is set manually. In the

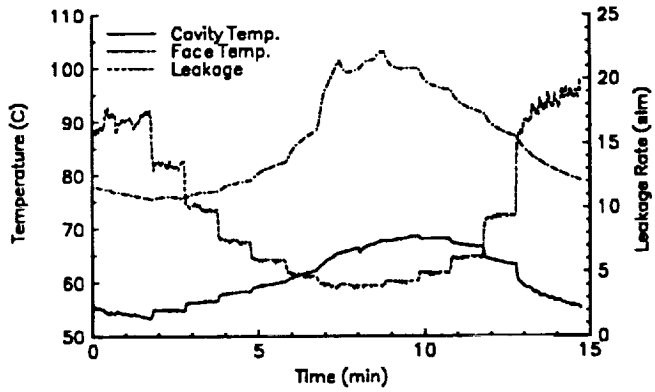

Figure 9 Temperature histories, steady state test.

transient tests, described below, the voltage is set by a closed loop control system based on a proportional, integral, derivative (P.I.D) control algorithm (6). The feedback to the control system is either the leakage rate of the seal (measured by the electronic flow meter in the air supply line) or the carbon face temperature (measured by the embedded thermocouple). The output of the control system is the voltage applied to the piezoelectric crystal. The purpose of the control system is to hold either the leakage rate or the face temperature at a setpoint value.

To determine the behavior of the electronically controlled mechanical seal under transient operating conditions, the seal

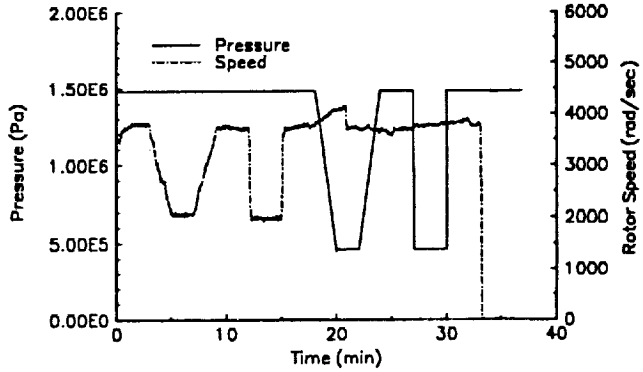

Figure 10 Duty cycle for transient tests (7).

has been subjected to the duty cycle shown in figure 10. Following startup, with a cavity pressure of 1.48×10^6 Pa, the seal initially operates for approximately three minutes with the same cavity pressure and a rotational speed of 3770 rad/sec. It then experiences a ramp decrease in speed to 2000 rad/sec, followed by a ramp increase back to 3770 rad/sec. Next it is subjected to a step decrease in speed to 2000 rad/sec, and a step increase in speed back to 3770 rad/sec. Following these speed transients, the speed is held approximately constant, and the seal experiences similar pressure transients: a ramp decrease (to 4.46×10^5 Pa) and increase, and a step decrease (to 4.46×10^5 Pa) and increase. The duty cycle is completed with a shutdown at constant pressure.

Figure 11 shows the results of a transient test in which the leakage rate is used as the feedback signal, with a setpoint

leakage rate of 12 slm. Thus, in this test the control system is attempting to control the leakage rate. From figure 11 it is

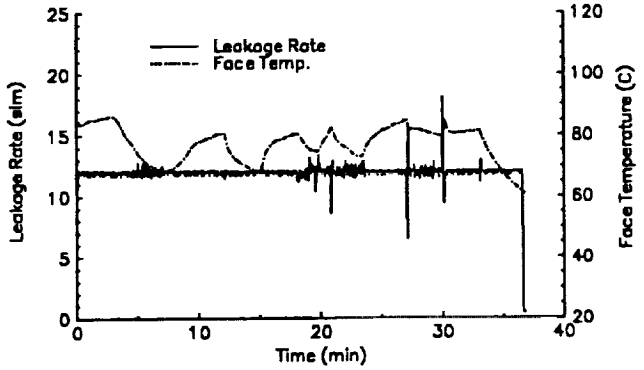

Figure 11 Transient test, controlled leakage rate (7).

seen that this control is very successful. Except for a few small spikes, the leakage rate is held close to the set point value. The largest spikes occur as a result of the step changes in pressure. However, since these are of very short time duration, they do not represent a significant change in total leakage (the integral of the leakage rate with time). It is also seen that the face temperature varies, but remains below 85 C, which is well within the temperature limits of the seal components.

The temporal history of the voltage (applied to the actuator) during the above transient test is contained in figure

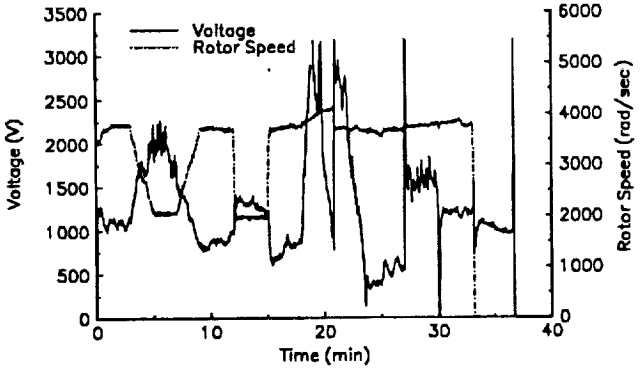

Figure 12 Voltage and speed vs. time, transient test with controlled leakage rate (7).

12. Also shown is the rotational speed, for reference. From the voltage plot, it is seen that the control system is very active, responding to the changes in both speed and cavity pressure.

Figure 13 shows the results of a transient test in which the face temperature is controlled. The feedback signal to the control system is the face temperature, and the setpoint temperature is 80 C. From this figure it is seen that the control system holds the face temperature very close to the setpoint. However, it is also seen that the leakage rate exhibits large variations, from 2 to 16 slm. The large reductions in leakage rate are undesirable, since they increase the risk of face contact. It is therefore believed that the previous control

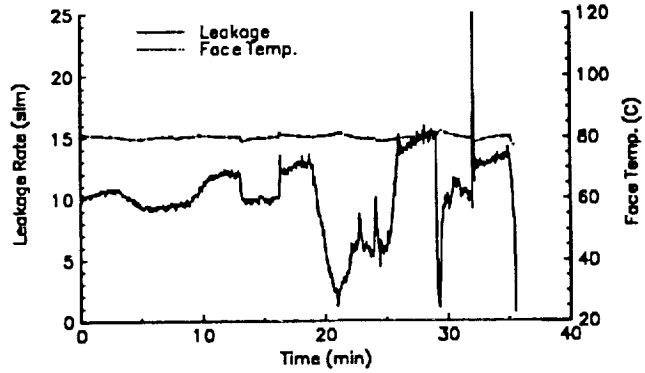

Figure 13 Transient test, controlled face temperature (7).

scheme, i.e., that in which the leakage rate is controlled, is superior.

The history of the applied voltage, during the test of figure 13, is shown in figure 14. It is seen that the control system is again quite active, responding to the changes in speed and pressure, as was the case in the previous test (controlled leakage rate).

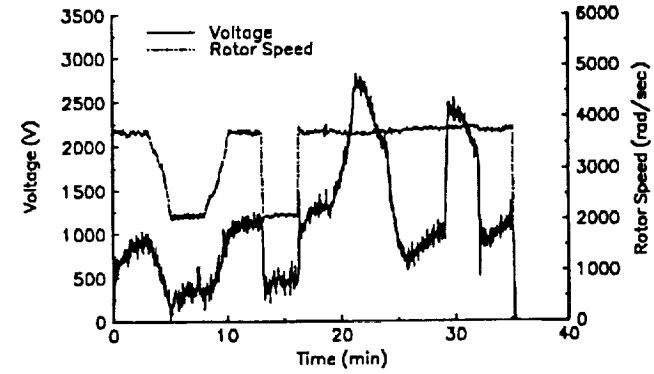

Figure 14 Voltage and speed vs. time, transient test with controlled face temperature (7).

SUMMARY AND CONCLUSIONS

The work described above has demonstrated that an electronically controlled mechanical seal, of a size and configuration suitable for aerospace applications, can be built. Steady state laboratory tests have shown that the leakage rate of the seal can be adjusted over a wide range, utilizing the available range of applied voltage. Transient tests have shown that either the leakage rate or the face temperature can be held close to a setpoint, by utilizing a closed loop control system. The results of the latter tests also suggest that control of the leakage rate is preferable, if it is desired to minimize the probability of face contact.

It should be noted that no attempt has been made to simulate the actual temperatures that occur in the demonstration application, i.e., in the purge gas seal assembly of a liquid oxygen turbopump. Therefore additional research is required before this concept can be applied to an operating

device. In particular, the seal design and materials, piezoelectric actuator, and control algorithm must be modified to handle the expected temperatures and temperature gradients.

Another area requiring additional work involves the prevention of electrical breakdown. For safety reasons, it is necessary to assure that electrical breakdown can never occur. There are two approaches to this problem. The first is to use a nonconducting controllable face holder (as was done in the present study) together with a nonconducting conformal coating completely encasing the piezoelectric crystal, to prevent breakdown. A second approach is to replace the piezoelectric crystal with a deformable hydraulic cell, and utilize an electrohydraulic control system instead of the electronic system of the present study.

ACKNOWLEDGEMENTS

This work has been supported by the National Aeronautics and Space Administration, Lewis Research Center, under Grant NAG 3-974. The NASA Technical Officer has been M. P. Proctor. The authors wish to acknowledge the Pure Carbon Company, who supplied the carbon graphite seal faces.

REFERENCES

1. Salant, R.F., Miller, A.L., Kay, P.L., Kozlowski, J., Key, W.E. and Algrain, M.C., "Development of an Electronically Controlled Mechanical Seal," in *Proc. 11th Intl. Conf. Fluid Sealing*, Nau, B.S., ed., BHRA, Cranfield, UK (1987), pp. 576-595.

2. Heilala, A.J. and Kangasniemi, A., "Adjustment and Control of a Mechanical Seal Against Dry Running and Severe Wear," in *Proc. 11th Intl. Conf. Fluid Sealing*, Nau, B.S., ed., BHRA, Cranfield, UK (1987), pp. 548-575.

3. Salant, R.F., Giles, O. and Key, W.E., "Design of Controllable Mechanical Seals," in *Tribological Design of Machine Elements*, Dowson, D., ed., Elsevier, Amsterdam, The Netherlands (1989), pp. 47-55.

4. Etsion I., Palmor, Z. and Harari, N., "Feasibility Study of a Controlled Mechanical Seal," *Lubr. Eng.*, 47, 8, pp. 621-625 (1991).

5. Salant, R.F., Wolff, P.J. and Navon, S., "Electronically Controlled Mechanical Seal for Aerospace Applications - Part I: Design, Analysis and Steady State Tests," *Tribology Transactions*, 37, 1 (1994).

6. Wolff, P.J., "Experimental Investigation of an Actively Controlled Mechanical Seal," Georgia Institute of Technology, Atlanta, Ga., Ph.D. Thesis (1993).

7. Wolff, P.J. and Salant, R.F., "Electronically Controlled Mechanical Seal for Aerospace Applications - Part II: Transient Tests," submitted to *Tribology Transactions*.